Chiroptical Activity in Silver Cholate Nanostructures Induced by the Formation of Nanoparticle Assemblies

ARTICLE *in* THE JOURNAL OF PHYSICAL CHEMISTRY C · MAY 2013

Impact Factor: 4.77 · DOI: 10.1021/jp400993j

7 AUTHORS, INCLUDING:

Hui Zhang
Rice University
39 PUBLICATIONS **415** CITATIONS
SEE PROFILE

Alexander O Govorov
Ohio University
144 PUBLICATIONS **4,752** CITATIONS
SEE PROFILE

THE JOURNAL OF PHYSICAL CHEMISTRY C

Article

pubs.acs.org/JPCC

Chiroptical Activity in Silver Cholate Nanostructures Induced by the Formation of Nanoparticle Assemblies

Muriel E. Layani,[†] Assaf Ben Moshe,[†] Maxim Varenik,[‡] Oren Regev,[‡] Hui Zhang,[§] Alexander O. Govorov,[§] and Gil Markovich*[,†]

[†]School of Chemistry, Raymond and Beverly Sackler Faculty of Exact Sciences, Tel Aviv University, Tel Aviv 69978, Israel

[‡]Department of Chemical Engineering and The Ilse Katz Center for Meso and Nanoscale Science and Technology, Ben Gurion University of the Negev, 84105 Beer Sheva, Israel

[§]Department of Physics and Astronomy, Ohio University, Athens, Ohio 45701, United States

Supporting Information

ABSTRACT: We report on an interesting mechanism of inducing chiroptical response at plasmonic silver nanoparticles (NPs) through the formation of plasmonic hot spots in small metal-NP−chiral-surfactant assemblies. Circular dichroism (CD) was measured at the surface plasmon resonance of cholate-coated silver nanostructures (AgCT) in the visible region of the spectrum. Low temperature cryogenic transmission electron microscopy (cryo-TEM) micrographs of the AgCT nanostructures in solution reveal small assemblies of silver NPs. Upon pH increase these assemblies are separated into individual NPs, and the induced plasmonic CD vanishes. This process was monitored via spectroscopy (CD and absorption), cryo-TEM, small-angle X-ray scattering (SAXS), and dynamic light scattering (DLS) measurements. The synthesis of well-separated AgCT NPs, which was performed with a large excess of sodium cholate (NaCT), also did not show any chiroptical effects. We interpret and model the formation of strong CD signals in the visible range in terms of the molecule−plasmon interaction in plasmonic hot spots formed in nanoparticle aggregates. Importantly, this study of the chiral induction, transfer to the visible range, and local field enhancement offers very attractive possibilities for sensing and detection of chirality of small amounts of molecules using visible light.

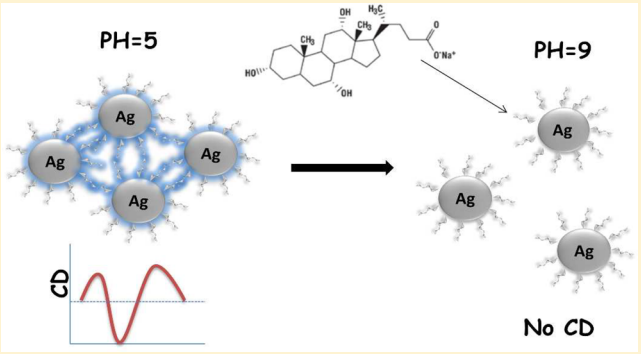

INTRODUCTION

Chirality, a widely studied property in chemistry and biology, appears in structures that are not superimposable with their mirror image (also called enantiomers). Each enantiomer is optically active, as it will interact in a different manner with linearly or circularly polarized light.

A useful technique to measure chiroptical effects is CD spectroscopy.[1,2] CD is the measure of the differential absorption between left- and right-handed circular polarizations of the incident light passing through the specimen. Chirality in metal clusters protected by a chiral molecular coating was first detected by the appearance of a CD signal at wavelengths that were typically on the red side of the absorption of the molecules capping the clusters and corresponded to transitions between metal core electronic states.[3] There are several possible mechanisms for this phenomenon, which were suggested in the past:[3] (1) The metal core becomes chiral because of the influence of chiral ligand molecules capping the cluster. (2) A chiral pattern is formed by the capping ligands on the surface of the achiral metal core. (3) Chirality is induced by electronic interaction between the chiral ligands and the achiral metal core electrons. Many studies were performed in the past, both experimental[4−8] and theoretical,[9] in an attempt to understand the mechanism leading to the metal chiroptical properties in different metal−surfactant systems at the nanometric scale.

In the present study, AgCT nanostructures were synthesized using a NaCT chiral template. NaCT is the sodium salt of the cholic bile acid. The bile acids are biologically the most important detergent-like molecules. They solubilize the insoluble components of bile, such as lecithin and cholesterol, and aid in digestion by removing the products of pancreatic hydrolysis (monoglycerides and fatty acids).[10] Bile salts, such as NaCT, are amphiphilic detergent-like molecules. The pH value is an important factor influencing the solubility of cholic acid and its sodium salt in water. NaCT and its derivatives are used for a variety of studies as biosurfactants[11] and in metal cholate systems.[12−14]

Special Issue: Ron Naaman Festschrift

Received: January 29, 2013
Revised: March 27, 2013
Published: April 19, 2013

We show here that the AgCT nanostructures exhibit chiroptical activity in the visible region of the spectrum (via CD spectra), coincident with the silver NP surface plasmon resonance. It is further demonstrated that the induction of CD is caused by the formation of small NP assemblies, since separating these assemblies into individual NPs causes the plasmonic CD spectrum to vanish. This suggests the formation of hot plasmonic spots in gaps between the silver NPs, which enhance the chiroptical response of the NaCT structures and transfer it to the silver plasmon region of the spectrum.

EXPERIMENTAL METHODS

Chemicals. All reagents used for the AgCT synthesis, including silver nitrate (99%), sodium cholate (99%), and sodium borohydride (99%) were purchased from Sigma-Aldrich and used without any further purification. All water used was ultrapure (18 MΩ·cm), obtained from a USF ELGA UHQ system.

Synthesis. For the synthesis of the AgCT nanostructures, aqueous solutions of silver nitrate (300 μL, 10 mM) and sodium cholate (300 μL, 10 mM) were added to 2.4 mL of water and left for ∼1 h in the dark. This was followed by the addition of sodium borohydride (30 μL, 100 mM) under vigorous stirring. For the pH adjustments we used 1 M solutions of sodium hydroxide and nitric acid.

Spectroscopic Measurements. Absorption and CD measurements were performed on an Applied Photophysics Chirascan CD spectrometer. For the baseline we used ultrapure water. The samples were diluted until the peak absorbance was ∼1.

TEM Studies. Cryo-TEM images were collected by a FEI Tecnai 12 G2 (equipped with a Gatan 794 CCD camera) operating at 120 kV. The samples were prepared using a controlled environment vitrification system. A drop of the sample was deposited on a plasma discharged copper TEM grid (30 s, plasma cleaner PDC-32G, Harric Plasma), coated with a holey carbon film (lacey substrate 300 mesh, Ted Pella, Ltd.). The grid was blotted to remove excess fluid using a Vitrobot (FEI), resulting in a thin film (20−300 nm) of the solution suspended over the holes of the grid. The samples were vitrified by rapid plunging into liquid ethane at its freezing point. The vitrified samples were then transferred to a cryoholder (Gatan model 626) and examined below −178 °C. The micrographs were analyzed and enhanced by "Digital Micrograph 3.6" software.

SAXS Experiments. A SAXSLAB GANESHA 300-XL was used to measure the small-angle X-ray scattering. Cu Kα radiation was generated by a Genix 3D Cu source (operated at 50 kV and 6 mA) with an integrated monochromator, three-pinhole collimation, and a two-dimensional Pilatus 300 K detector. The distance between the sample and detector was 350 mm. The q range was between 0.012 and 0.67 Å^{-1}. $q = (4\pi \sin\theta)/\lambda$, where λ is the incident X-ray wavelength and 2θ is the scattering angle.

DLS Measurements. All DLS measurements were performed using a Malvern Instruments Nano ZS system. All samples were diluted to the same concentrations measured in the CD and absorption experiments.

RESULTS AND DISCUSSION

Figure 1 displays the evolution of the absorbance and CD spectra of a 1 mM cholate solution with addition of silver ions

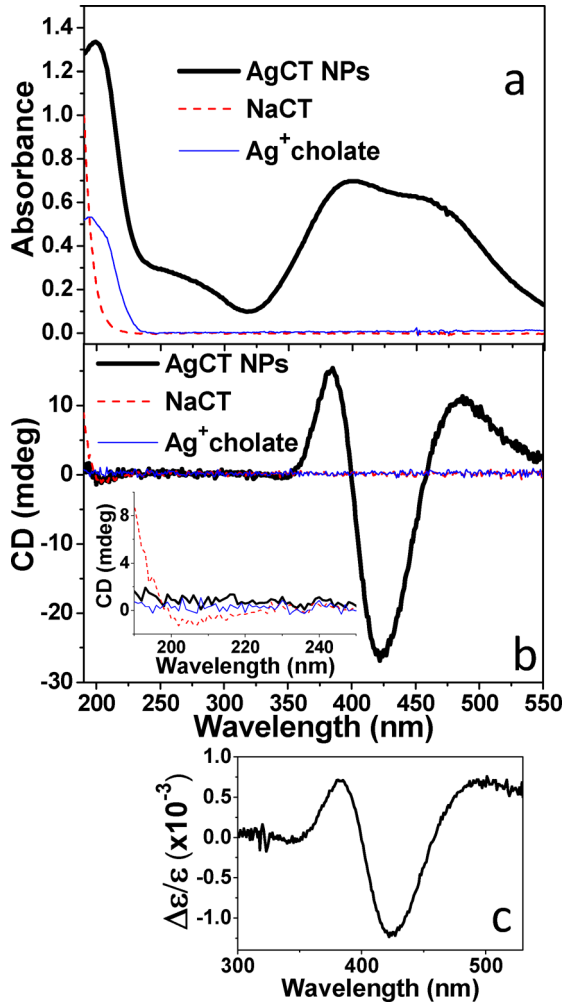

Figure 1. (a) Absorbance and (b) CD spectra of NaCT solution, not reduced (Ag^+-cholate) and reduced (AgCT) nanostructures, at pH ≈ 5. The inset of (b) shows the expanded CD spectra at the molecular absorption region around 200 nm. (c) AgCT nanostructures' dissymmetry spectrum.

(silver/cholate molar ratio of 1:1) and after the reduction of the silver ions by sodium borohydride to form silver nanoparticles. The absorption curve of the AgCT nanoparticles was measured about 1 h after the addition of the borohydride (Figure 1a). It shows a complex plasmon resonance line shape, with two peaks apparent at ∼390 and ∼460 nm. Figure 1b displays the corresponding Ag plasmonic CD spectrum, showing a complex line shape spanning the full width of the absorption line, with two positive peaks at ∼380 and ∼480 nm and a negative peak at ∼425 nm.

A large variety of silver/cholate molar ratios, including low and high concentrations, was studied. The 1:1 molar ratio was found as the optimum to give the largest CD signal at the silver plasmonic region of the spectrum. The 1:20 molar ratio was found to be the threshold ratio at which the CD induction completely disappeared.

The dissymmetry spectrum is presented in Figure 1c. The dissymmetry factor is a dimensionless measure of the strength of optical activity, which is independent of concentration. It is the ratio of differential-to-total molar absorption coefficient: $\Delta\varepsilon/\varepsilon$ (or $\Delta A/A$). We can compare the values in the peak of the dissymmetry spectrum to values achieved in former studies,

dx.doi.org/10.1021/jp400993j | J. Phys. Chem. C 2013, 117, 22240−22244

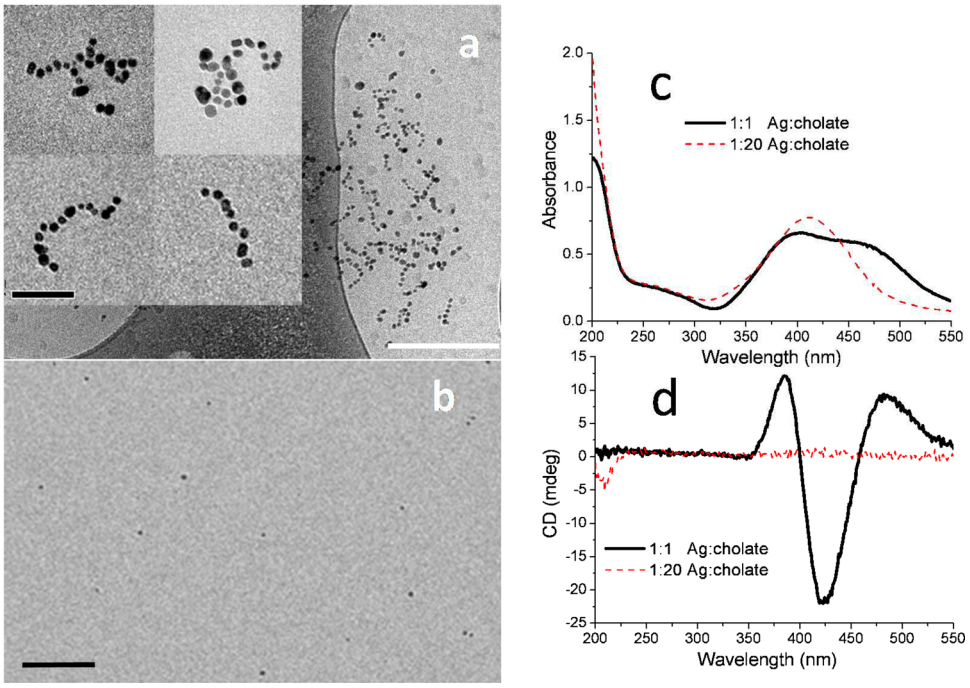

Figure 2. (a) Cryo-TEM micrographs of AgCT assemblies obtained from 1:1 Ag/NaCT solution at pH ≈ 5 (scale bar = 0.2 μm, inset scale bar = 50nm). (b) Cryo-TEM image of AgCT NPs prepared from 1:20 Ag/NaCT molar ratio (scale bar = 50 nm). (c) Absorption and (d) CD spectra of AgCT NPs synthesized with 1:20 molar ratio of $AgNO_3$/NaCT compared to the spectra of AgCT NPs synthesized with 1:1 molar ratio of Ag/NaCT.

such as the work of Yao and co-workers in which they present size dependence of the maximum anisotropy factors of penicillamine-capped silver and gold nanoclusters.[8] In their work they show a relatively large dissymmetry factor of ∼0.0015 for penicillamine-capped silver nanoclusters with ∼1 nm core size. The dissymmetry was found to strongly decrease with the increase in cluster size, indicating a localized surface-sensitive CD induction mechanism. In the present case a dissymmetry factor on the order of 10^{-3} is obtained for larger silver nanoparticles of ∼10 nm, which together with the complex plasmonic line shape indicates a different CD induction mechanism.

When looking at the UV region of the absorption and CD spectra (inset of Figure 1b), where we can find information on the molecular absorption lines, one can see that the molecular CD signal vanishes on creating the AgCT nanostructures. A possible explanation for this effect will be presented later, in the discussion of a model for the chiroptical effects.

Figure 2a presents the cryo-TEM micrographs of the 1:1 AgCT nanostructures in solution. The AgCT NPs are arranged in small assemblies, primarily linear chains, which are self-assembled in the solution. The native AgCT solution had pH ≈ 5, which is also the cholic acid's pK_a value.[10] Cholate molecules tend to form high aspect ratio structures on assembly in water when neutralized. The carboxylate groups extending from the side of the cholate molecules have a high affinity toward silver surfaces (probably to the thin oxide/hydroxide layer covering the surface). Thus, it is believed that these elongated structures are the scaffold on which the silver particle chains form. Image analysis of the cryo-TEM micrographs provided an average particle diameter of 8 ± 3 nm (averaging over 311 particles) and an average wall-to-wall separation between NP surfaces in the assemblies of 3 ± 2 nm (see Supporting Information, Figures S2 and S3, for more information).

The AgCT NPs−cholate structures were also studied by SAXS, and the distance distribution function analysis of this data (see Supporting Information, Figure S4) yielded average particle diameter of ∼10 nm and wall to wall distance of about ∼1 nm. Thus, the results from cryo-TEM and SAXS are rather similar.

The aggregation-induced plasmonic splitting and CD induction phenomena are unique to the particular synthesis conditions described above. Using 20 times higher NaCT concentration than that used above, we were able to synthesize small, well-separated AgCT NPs that showed no chiroptical activity in the visible range of the spectrum nor a double plasmonic absorption peak (see Figure 2c,d). Figure 2b presents a cryo-TEM image for these NPs, which clearly shows well-separated NPs (≤10 nm) without formation of NP aggregates. The large AgCT concentration ratio that was used for this synthesis is probably the reason that no assemblies were formed, as cholate molecules tend to interact with one another to create different stacked structures, which could create a large separation between the NPs with negligible plasmonic interaction between the particles.

Zhang and Govorov have previously predicted a situation where plasmonic NP aggregates would create hot spots that would uniquely cause the appearance of plasmonic CD with complex line shapes.[15] This simple model, based on the Coulomb interaction between the plasmonic NP dimer and the molecular dipole, was applied to the current system, where the plasmonic CD was calculated for silver spheres with R = 5 nm separated at various distances (Figure 3). The cholate molecules were modeled as molecular dipoles having CD lines at 190 nm. More details of the calculation are given in Supporting Information. Figure 3 displays the features and the calculated plasmonic and molecular CD spectra for various d (wall-to-wall separation) values. An important point to note is

dx.doi.org/10.1021/jp400993j | J. Phys. Chem. C 2013, 117, 22240−22244

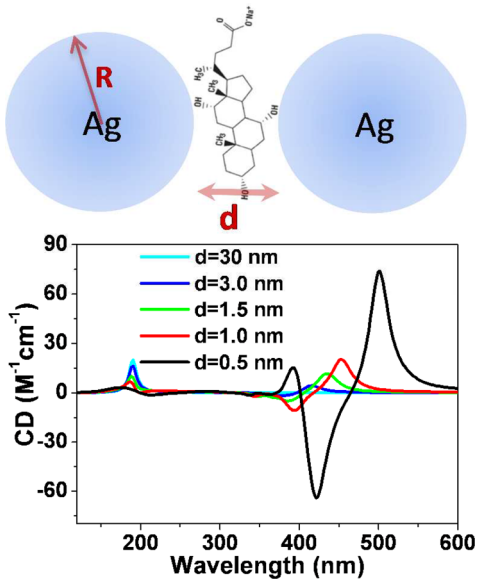

Figure 3. Model calculation of hot spot induced plasmonic CD: (top) geometry of the model; (bottom) calculated CD spectra for various *d* values and for a randomly oriented dipole of a chiral molecule.

the suppression and change in line shape of the molecular CD line at 190 nm with decreasing interparticle separation. In our model, this decrease of the natural CD signal comes mostly from the effect of broadening of the molecular resonance due to energy transfer to metal at small distances *d*. This may explain the fact that we do not see the molecular CD line in the experimental AgCT CD spectra (Figures 1b and 2d). The qualitative agreement of the model with the experimental data is satisfactory, as the model is very simple and only intended to grasp the mechanism leading to the appearance of plasmonic CD of NP aggregates with expected plasmonic hot spots.

Another theoretical study, which supports these results, was presented by Schatz and co-workers.[16] They calculated the plasmonic extinction spectra for individual Ag NPs and dimers. The spherical Ag NP dimers exhibit distinct dipole and quadrupole plasmon resonance features. Gun'ko and co-workers showed a similar effect of CD signal arising due to aggregation effects in Au oligonucleotide systems.[17] They also suggest that this phenomenon may arise from the formation of hot plasmonic spots in aggregates and from the Coulomb interaction between the chiral molecules and the metal plasmons.

Consequently, the two absorption peaks obtained for 1:1 Ag/NaCT at ~390 and ~460 nm can be related to dipole and quadrupole plasmon resonance features resulting from the formation of dimers. In particular, the absorption peak at 390 nm is primarily the result of this splitting rather than belonging to uncoupled silver particles. This is confirmed by the appearance of a strong plasmonic CD peak at ~380 nm, practically overlapping the ~390 nm absorption (see also Figure 3 in ref 15 and Figure S-1 in its supplementary material). The isolated Ag particles do not show this CD signature.

When the pH of the reduced AgCT structures for the Ag/NaCT 1:1 sample is raised, the assemblies observed at the cryo-TEM images (Figure 2a) disappeared and the cryo-TEM image of the solution at pH 9 contains only separated AgCT NPs (seen in Figure 4c). The plasmonic CD peaks vanished together with the ~460 nm split plasmonic absorption peak on increasing pH from 5 to 9 as displayed in Figure 4a,b. Analysis

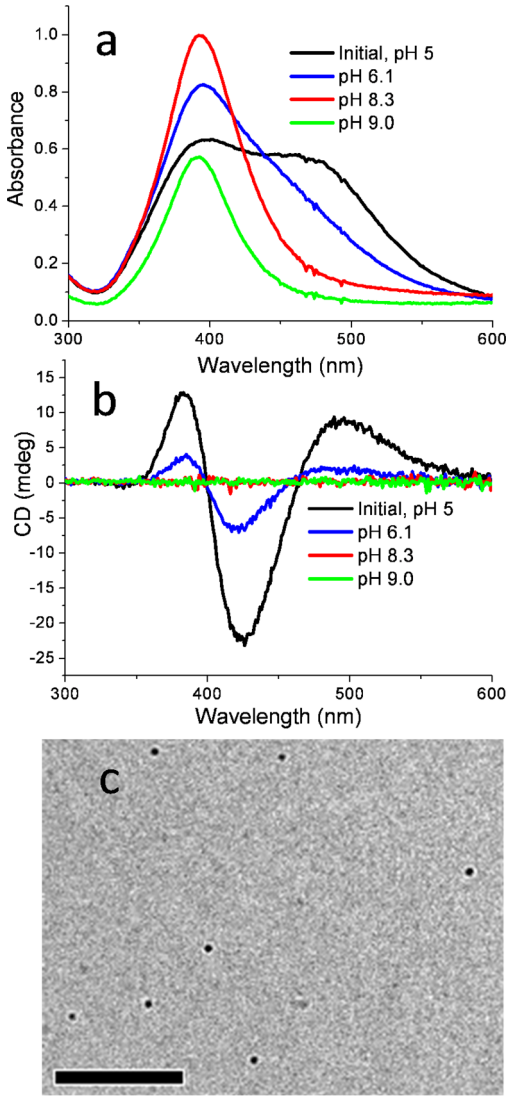

Figure 4. (a) Absorption and (b) CD spectra of AgCT NPs monitored during the raising of pH from 5 to 9. (c) CryoTEM image of AgCT NPs at pH 9 (scale bar = 0.2 μm).

of these cryo-TEM images yielded an average particle diameter of 13 ± 3 nm (Supporting Information, Figure S2), and the typical distance between particles in an assembly was >100 nm. Moreover, DLS measurements of the above-mentioned solutions presented a similar picture where the measured hydrodynamic diameter was reduced to ~20 nm as the pH was raised above 6 (Table 1). The raising of the pH values causes deprotonation of the carboxylate groups (at pH > 5), breaking hydrogen bonds, charging of the cholate molecules, and

Table 1. DLS Measurements of AgCT NPs at Different pH Values

pH	hydrodynamic size (DLS) [nm]
5.0	~260
5.5	~64
6.1	~23
7.7	~21
7.9	~24
8.3	~18

dx.doi.org/10.1021/jp400993j | J. Phys. Chem. C 2013, 117, 22240−22244

consequently breaking of the assemblies into separate NPs. The shrinking of aggregate size occurs when the pH crosses the pK_a of the cholic acid of ~5.2. These results prove that the silver NPs were not intrinsically chiral.

After the pH was increased to only 6.8, partly reducing the magnitude of the plasmonic CD line, the CD signal could be slightly re-formed with decrease of the pH back to 5 (Supporting Information, Figures S5). At higher pH values, when the plasmonic CD completely vanishes, the aggregates could not be re-formed. It is clear that the AgCT complex formed before the reduction creates a specific arrangement of the silver cholate that produced the NP aggregates and induces the chiroptical response at the silver NPs. Such an arrangement apparently cannot be recreated when the metal is reduced and aggregates are broken.

This work presents an intriguing plasmonic CD induction effect that is different from the previous CD induction effects described in the literature, excluding ref 17, which also exhibited aggregation related plasmonic CD. In the present work, the CD induction occurred only when the metal NPs formed aggregates at low pH when they are minimally charged. This CD signal could be switched off when the NPs were separated but still coated with (charged) cholate molecules. This fact, together with the complex plasmonic CD line shape corresponding to the NP aggregates, indicates that the formation of the NP aggregates is essential for attaining the high dissymmetry values in the plasmonic CD, as predicted by Govorov and co-workers. However, it cannot be ruled out that in addition to the plasmonic hot spots formed in the aggregates, an additional aspect related to pH change is the change in molecular orientation with respect to the NP surfaces which may also affect the magnitude of the induced plasmonic CD. Another possibility, that the NP aggregates form chiral superstructures, as in the helical assemblies recently formed using DNA origami,[18] is not supported by the TEM images of the aggregates, which show linear chains (see Figure 2a).

CONCLUSION

In summary, we have reported on an interesting mechanism of inducing chiroptical response at silver NPs through the formation of plasmonic hot spots in small AgCT assemblies. The dissymmetry values received for the AgCT assemblies are relatively high when compared to dissymmetry factors of silver nanoclusters in the literature. This chirality induction mechanism could be useful as a surface enhanced CD technique for probing small quantities of chiral molecules.

ASSOCIATED CONTENT

Supporting Information

Cryo-TEM image analysis, SAXS results, additional CD data, and details of model calculation. This material is available free of charge via the Internet at http://pubs.acs.org.

AUTHOR INFORMATION

Corresponding Author

*Phone: 972-3-640-6985. E-mail: gilmar@post.tau.ac.il.

Notes

The authors declare no competing financial interest.

ACKNOWLEDGMENTS

This research was supported by The Israel Science Foundation Grant No. 172/10, the James Frank program on light−matter interaction, and NSF (U.S.). A.B.M. was supported by an Adams fellowship. Dr. Ronit Bitton is kindly acknowledged for helpful discussions on SAXS experiments and analysis.

REFERENCES

(1) Berova, N., Nakanishi, K., Woody, R. W., Eds. *Circular Dichroism: Principles and Applications*, 2nd ed.; Wiley-VCH: New York, 2000.
(2) Ambilino, D. B., Ed. *Chirality at the Nanoscale: Nanoparticles, Surfaces, Materials and More*; Wiley-VCH: Weinheim, Germany, 2009.
(3) Schaaff, T. G.; Whetten, R. L. Giant Gold-Glutathione Cluster Compounds: Intense Optical Activity in Metal-Based Transitions. *J. Phys. Chem. B* **2000**, *104*, 2630−2641.
(4) Nishida, N.; Yao, H.; Kimura, K. Chiral Functionallization of Optically Inacttive Monolayer-Protected Silver Nanoclusters by Chiral Ligand-Exchange Reactions. *Langmuir* **2008**, *24*, 2759−2766.
(5) Yao, H.; Saeki, M.; Kimura, K. Induced Optical Activity in Boronic-Acid Protected Silver Nanoclusters by Complexation with Chiral Fructose. *J. Phys. Chem. C* **2010**, *114*, 15909−15915.
(6) Shemer, G.; Krichevski, O.; Markovich, G.; Molotsky, T.; Lubitz, I.; Kotlyar, A. B. Chirality of Silver Nanoparticles Synthesized on DNA. *J. Am. Chem. Soc.* **2006**, *128*, 11006−11007.
(7) Molotsky, T.; Tamarin, T.; Ben Moshe, A.; Markovich, G.; Kotlyar, A. B. Synthesis of Chiral Silver Clusters on a DNA Template. *J. Phys. Chem. C* **2010**, *114*, 15951−15954.
(8) Nishida, N.; Yao, H.; Ueda, T.; Sasaki, A.; Kimura, K. Synthesis and Chiroptical Study of D/L-Penicillamine-Capped Silver Nanoclusters. *Chem. Mater.* **2007**, *19*, 2831−2841.
(9) Govorov, A. O.; Fan, Z.; Hernandez, P.; Slocik, J. M.; Naik, R. R. Theory of Circular Dichroism of Nanomaterials Comprising Chiral Molecules and Nanocrystals: Plasmon Enhancement, Dipole Interactions, and Dielectric Effects. *Nano Lett.* **2010**, *10*, 1374−1382.
(10) Nair, P. P., Kritchevsky, D., Eds. *The Bile Acid: Chemistry, Physiology and Metabolism*; Plenum Press: New York, 1971.
(11) Galantini, L.; Leggio, C.; Jover, A.; Meijide, F.; Pavel, N. V.; Soto Tellini, V. H.; Vazquez Tato, J.; Di Leonardo, R.; Ruocco, G. Kinetics of Formation of Supramolecular Tubules of a Sodium Cholate Derivative. *Soft Matter* **2009**, *5*, 3018−3025.
(12) Qiao, Y.; Lin, Y.; Wang, Y.; Yang, Z.; Liu, J.; Zhou, J.; Yan, Y.; Huang, J. Metal-Driven Hierarchical Self-Assembled One-Dimensional Nanohelices. *Nano Lett.* **2009**, *9*, 4500−4504.
(13) Qiao, Y.; Wang, Y.; Yang, Z.; Lin, Y.; Huang, J. Self-Templating of Metal-Driven Supramolecular Self-Assembly: A General Approach toward 1D Inorganic Nanotubes. *Chem. Mater.* **2011**, *23*, 1182−1187.
(14) Chandirasekar, S.; Dharanivasan, G.; Kasthuri, J.; Kathiravan, K.; Rajendiran, N. Facile Synthesis of Bile Salt Encapsulated Gold Nanoparticles and Its Use in Colorimetric Detection of DNA. *J. Phys. Chem. C* **2011**, *115*, 15266−15273.
(15) Zhang, H.; Govorov, A. O. Giant Circular Dichroism of a Molecule in a Region of Strong Plasmon Resonances between Two Neighboring Gold Nanocrystals. *Phys. Rev. B* **2013**, *87*, 075410.
(16) Hao, E.; Schatz, G. C. Electromagnetic Fields around Silver Nanoparticles and Dimers. *J. Chem. Phys.* **2004**, *120*, 357−366.
(17) Gerard, V. A.; Gun'ko, Y. K.; Defrancq, E.; Govorov, A. O. Plasmon-Induced CD Response of Oligonucleotide-Conjugated Metal Nanoparticles. *Chem. Commun.* **2011**, *47*, 7383−7385.
(18) Kuzyk, A.; Schreiber, R.; Fan, Z.; Pardatscher, G.; Roller, E. M.; Högele, A.; Simmel, F. C.; Govorov, A. O.; Liedl, T. DNA-Based Self-Assembly of Chiral Plasmonic Nanostructures with Tailored Optical Response. *Nature* **2012**, *483*, 311−314.